Immunobiology xxx (2015) xxx–xxx

Contents lists available at ScienceDirect

Immunobiology

journal homepage: www.elsevier.com/locate/imbio

A novel antibody targeting CD24 and hepatocellular carcinoma *in vivo* by near-infrared fluorescence imaging

Hua He [1], Xiaojie Tu [1], Juan Zhang*, Desmond Omane Acheampong, Li Ding, Zhaoxiong Ma, Xueyan Ren, Chen Luo, Zhiguo Chen, Tong Wang, Wei Xie, Min Wang*

State Key Laboratory of Natural Medicines (China Pharmaceutical University), School of Life Science & Technology, China Pharmaceutical University, Nanjing 210009, PR China

ARTICLE INFO

Article history:
Received 5 January 2015
Received in revised form 13 March 2015
Accepted 7 July 2015
Available online xxx

Keywords:
CD24
Monoclonal antibody
scFv
Tumor targeting
Near-infrared fluorescence imaging

ABSTRACT

Liver cancer is one of the most common malignant cancers worldwide. The poor response of liver cancer to chemotherapy has whipped up the interest in targeted therapy with monoclonal antibodies because of its potential efficiency. One promising target is cluster of differentiation 24 (CD24), which is known to beover-expressed on hepatocellular carcinoma (HCC), providing prospect for HCC targeted diagnosis and therapy. In this study we developed a novel CD24 targeted monoclonal antibody G7mAb based on hybridoma technology and then generated a single-chain antibodyfragment (scFv) G7S. Firstly, ELISA, western blot, and flow cytometry assays demonstrated specific binding of CD24 by G7mAb and G7S. Further, G7mAb was demonstrated to have similar binding capacity as ML5 (a commercial Anti-CD24 Mouse Antibody) inimmunohistochemical assay. Further more, a near-infrared fluorescent dye multiplex probe amplification (MPA) was conjugated to G7mAb and G7S to form G7mAb-MPA and G7S-MPA. The near-infrared fluorescence imaging revealed that G7mAb and G7S aggregate in CD24 + Huh7 hepatocellular carcinoma xenograft tissuevia specific binding to CD24 *in vivo*. In conclussion, G7mAb and G7S were tumor targeted therapeutic and diagnostic potentials *in vitro* and *in vivo* as anticipated.

1. Introduction

Hepatocellular carcinoma (HCC) is the most frequent form of primary liver cancer in adults, accounting for approximately 600,000 new cases per year worldwide (El-Serag and Rudolph, 2007). Historically, human cancers are treated mostly through radiotherapy, chemotherapy, and surgery. However, these cancer therapeutic options, especially chemotherapy and radiotherapy are usually associated with many adverse effects (Maor and Malnick, 2013). The HCC in particular has shown poor prognosis, low response rate to treatment, severe toxicity and high recurrence rates (Belnoue et al., 2004; Levin and Amos, 1995). Small and localized tumors are usually curable with surgery, however, most patients usually report with advanced condition at diagnosis, therefore surgery is not possible due to the underlying cirrhosis (Bruix and Sherman, 2005; Lorenz et al., 2000; Matar et al., 2009). This development therefore calls for novel strategies such as immunotherapy to address the limitations associated with chemotherapy and radiotherapy, knowing very well that surgery can not be relied upon always.

The immune system is known to play crucial role in the control of cancer and has essentially opened new therapeutic option which works by manipulating the immune system to eliminate malignant cancers (Berzofsky et al., 2004; Gilboa, 2004; Matar et al., 2009). Studies elsewhere on clinical trials have demonstrated clearly that immunotherapy is a potent option in the treatment of patients with HCC (Butterfield et al., 2007; Gao et al., 2007; Kobayashi et al., 2007; Peng et al., 2005). An aspect of immunotherapy referred to as targeted therapy, which include monoclonal antibodies and small molecule inhibitors have improved significantly the treatment of malignancies in recent times, providing

Abbreviations: ELISA, enzyme-linked immunosorbent assay; FACS, fluorescence activated cell sorter; FITC, fluorescein isothiocyanate; FBS, fetal bovine serum; HRP, horeradishperoxidase; IgG, immunoglobulin G; mAb, monoclonal antibody; scFv, single-chain antibody fragment.

* Corresponding authors at: State Key Laboratory of Natural Medicines, China Pharmaceutical University, 154#, Tong Jia Xiang 24, Nanjing 210009, PR China. Fax: +86 25 8327 1395.

E-mail addresses: juancpu@126.com (J. Zhang), minwang@cpu.edu.cn (M. Wang).

[1] The authors Hua He and Xiaojie Tu contributed equally to this work.

http://dx.doi.org/10.1016/j.imbio.2015.07.010
0171-2985/

potent alternative to the traditional cytotoxic chemotherapy and radiotherapy (Gerber, 2008). The main challenge to this therapy option is the difficulty in finding tumor-specific targets (Mitchell, 2011).

One promising target is Cluster of differentiation 24 (CD24), which is a glycosylphosphatidylinositol-linked cell surface glycoprotein encoded in human by the CD24 gene (Hough et al., 1994; Soave et al., 2013; Weichert et al., 2005). It has been identified as a P-selectin ligand and adhesion receptor for platelets and activated endothelial cells (Kristiansen et al., 2004; Lim, 2005; Soave et al., 2013). CD24 is over-expressed in many human tumors, and it is known to be over-expressed on HCC (Huang and Hsu, 1995), providing prospect for HCC targeted therapy. Studies on the use of CD24 over-expressed in prognosis, diagnosis, and targeted therapy on various cancerous conditions have captured the attention of scientists in recent times due to the prospects (Deng et al., 2012; Karimi-Busheri et al., 2013; Liu et al., 2013; Schostak et al., 2006).

In this current study, we developed CD24 targeted monoclonal antibody G7mAb through hybridoma technology and further generated single-chain antibody fragment (scFv) against CD24 (G7S) based on G7mAb, and investigated their diagnostic and targeted therapy features on HCC *in vitro* and *in vivo*. The antibodies exhibited both tumor targeted therapeutic and diagnostic potentials *in vitro* and *in vivo.*

2. Materials and methods

2.1. Cell culture and animals

The murine myeloma cell line Sp2/0-Ag14 preserved in our lab was cultured in DMEM medium (high glucose), supplemented with 10% (v/v) fetal bovine serum (FBS). The human hepatoma cell line Huh7 and the human colon cancer cell line HCT116 preserved in our lab were cultured in RPMI 1640 medium containing 10% (v/v) FBS. The human colon cancer cell line HT29 preserved in our lab was cultured in McCoy'5A medium containing 10% (v/v) FBS. Cell culture media and supplements used in this study were purchased from Life technologies (Basel, Switzerland). The animals used in this study were purchased from Yangzhou University.

2.2. Construction of the expression system E. coli *BL21 (DE3)/pGEX-CD24*

The appropriate cDNA of the CD24 was obtained from the GENEBANK (accession number: 100133941). The expression system *Escherichia coli* DH5α/pGEX-CD24 was constructed by SANGON (Shanghai, China). The expression system *E. coli* BL21 (DE3)/pGEX-CD24 was then constructed by extracting the recombinant vector (Plasmid Minipreparation Kit, Biomiga, USA) and transforming into a more suitable *E. coli* strain, BL21 (DE3). The positive clones were then selected from Luria–Bertani (LB) plates containing appropriate anbiotics (100 μg/ml Ampicillin) and confirmed with colony PCR and sequencing (SANGON, Shanghai, China).

2.3. Expression and purification of the CD24

Positive clone of CD24 was selected and cultured in 10 ml of liquid LB medium containing 100 μg/ml ampicillin overnight at 37 °C. It was then subcultured (1:100) in 500 ml fresh medium and incubated for about 2.5 h at 37 °C. The expression of CD24 was then induced with 0.1 mM isopropyl-thio-b-D-galactoside (IPTG) and incubated for further 6 h at 37 °C. The bacteria was harvested and suspended in PBS (w(g)/v(ml) = 1/20; pH 7.4). It was then treated with lysozyme (1 mg/ml) (incubated 30 min on ice), 10 ml 0.2% Triton X-100, 5 μg/ml DNase (incubated at 4 °C for 10 min). The supernatant was then collected (4 °C, 3000 g, 30 min) and treated with DTT (1 mmol/L final concentration). The target protein GST-CD24 was verified by western blot assay, then purified with affinity chromatography employing GSTrapFF (1 ml) column (GE Healthcare, Buckingghamshire, UK). A successful purification was verified with SDS-PAGE.

2.4. Preparation of murine anti-CD24 antibody G7mAb

50 μg GST-CD24 and an equal volume of Quick Antibody adjuvant (Biodragon-Immunotech, Beijing, China) were intramuscularly injected into 6-week-old female BALB/c mice. Subsequencely, a booster immunization was conducted after 3 weeks in the same manner. Serum antibody titers were measured by indirect ELISA and the mouse with highest serum antibody titer was selected to be spleen donors for hybridoma generation. A final injection of 20 μg GST-CD24 and an equal volume of Quick Antibody adjuvant was given to the donor mouse 3 days before being sacrificed and the spleen removed. 5×10^8 spleenocytes were fused with 10^8 Sp2/0-Ag14 myolema cells using the PEG method and hyrodoma cells were selected in HAT medium (DMEM supplemented with 20% FBS, 10 mM sodium hypoxanthanine, 40 mM aminopterin, and 1.6 mM thymidine). Positive clones were selected using an indirect ELISA. Stable hybridoma cell line G7 secrecting anti-CD24 antibody G7mAb was obtained after three cycles of subcloning. The isotype of resoulting G7mAb was determined to be IgG1κ isotype using the isotyping kit (Proteintech Group Inc., China).

To produce anti-CD24 antibody G7mAb, hybidoma cells were injected intraperitoneally into liquid paraffin pretreated 8-week-old female mice with 10^6 cells per mouse. Approximately 7 days later, ascites were collected and applied onto protein G affinity chromatography cloum (GE Healthcare, Buckingghamshire, UK). A successful production and purification of G7mAb was confirmed with SDS-PAGE and western blot assay (HRP conjugated goat anti-mouse IgG (H + L); Millipore, USA).

2.5. Immunoblotting with G7mAb

Recombinant human CD24-Fc chemera (Sino Biological Inc., China) and recombinant human Fc (Sino Biological Inc., China) were loaded into different wells on two 15% (w/v) SDS–PAGE for electrophoresis and transferred onto two different polyvinylidenedifluoride (PVDF) membranes (Millipore, USA). Blotted membranes were placed in TBS buffer with 5% (w/v) skim milk at 37 °C for 2 h. One of the blotted membranes was incubated with G7mAb whereas the other was incubated with anti-Fc antibody (Sino Biological Inc., China) at 4 °C overnight. After washing with TBST and TBS, the membrane was incubated with HRP conjugated goat anti-mouse IgG (Millipore, USA) at room temperature for 1.5 h. After successive washing as described previously, the blots were treated with enhanced chemiluminescence (ECL) solution (Millipore, USA) and exposed in gel imaging systems (Bio-rad).

2.6. Friguet (Indirect ELISA) determination of G7mAb affinity

50 μL nine different concentrations of antigen (0, 3.19×10^{-11}, 2.55×10^{-10}, 2.05×10^{-9}, 1.62×10^{-8}, 1.30×10^{-7}, 1.04×10^{-6}, 8.32×10^{-6}, and 6.65×10^{-5} M) were mixed individually with 50 μl 10 pmol/L G7mAb, and incubated at 4 °C overnight. The mixtures were transferred and incubated for 1.5 h at 37 °C into the wells of a microtitration plate previously coated with CD24 peptide (SANGON, Shanghai, China). After washing with PBST and PBS, the bound immunoglublins were detected by adding HRP conjugated goat anti-mouse IgG (Millipore, USA). Visualization was achieved with TMB peroxidase substrate (BBI) and the absorbance at 450 nm with

Please cite this article in press as: He, H., et al., A novel antibody targeting CD24 and hepatocellular carcinoma *in vivo* by near-infrared fluorescence imaging. Immunobiology (2015), http://dx.doi.org/10.1016/j.imbio.2015.07.010

a reference 630 nm was read with Microplate Reader (Thermo Fisher Scientific Inc., USA).

2.7. Flow cytometry assays of G7mAb

The affinity of G7mAb to native CD24 over-expressed on Huh7 (Human hepatoma cell line) (Lee et al., 2011), HT29 (Human colon cancer cell line) (Shapira et al., 2011) and non-expressed HCT116 (Human colon cancer cell line) (Shapira et al., 2011) were assessed with flow cytometry. 5×10^5 of the respective cells per sample were suspended in PBS containing 5% FBS and incubated with 10 μg/ml G7mAb and with controls anti-CD24 antibody ML5 (a commercial Anti-CD24 Mouse Antibody, BD Pharmingen, USA) and isotype antibody in separate setups at 4 °C for 30 min. Cells were then incubated with FITC-conjugated goat anti-mouse IgG antibody (Signalway Antibody, USA) for another 30 min. Finally, the cells were washed and analyzed with a BD FACS flow cytometer.

2.8. Analysis of the G7mAb variable genes

Total RNA was extracted from 10^7 hybridoma cells at logarithmic phase with Total RNA Extractor kit (SANGON, Shanghai, China). With the RNA as temperate, cDNA was synthesized through RT-PCR with M-MuLV First Strand cDNA synthesis Kit (SANGON, Shanghai, China). The variable regions of the heavy and light chain were then amplified with degenerate PCR with published primers (Wang et al., 2000) and identified the product with agarose gel electrophoresis. Adenine at the 3-terminal of each fragment was achieved with polymerase chain reaction (PCR). The target genes were then cloned into *E. coli* DH5α *via* T-A Cloning assay and the positive clones screened with colony PCR and sequenced by Sangong Biotech (Shanghai, China). The Sp2/0-Ag14 myeloma cell lines might endogenously express aberrant Vκ. Therefore, to avoided the production of aberrant Vκ, we used the cross targeting CDR1 and CDR3 of the aberrant light chains, and screened by colony PCR. Finally, the protein sequences of VH and VL were loaded into the IMGT database and the CDR1-3 and FR1-4 of VH and VL analyzed with IMGT/V-QUEST Tool.

2.9. Preparation and purification single-chain antibody fragment of G7mAb

A single-chain antibody fragment of G7mAb (named G7S) by linking VH and VL with $(G_4S)_3$ linker and adding His-tag directly to the VL was desighed and synthesized after codon usage optimization. The correct DNA insertion was cloned into pET22b(+) vector and then transformed into *E. coli* BL21 (DE3). The expression of G7S was induced with IPTG and purified with immoblizedion affinity chromatography. The expression and purification was verified with SDS-PAGE and western blot assay (His-Tag mouse mAb, HRP conjugated goat anti-mouse IgG (H + L); Signalway Antibody, USA). Specific binding of CD24 *in vitro* was examined by ELISA and flow cytometry assays (Supplementary materials and methods).

2.10. Establishment and validation of CD24 overexpressed hepatocellular carcinoma xenograft model

Huh7 human liver cancer model: 6-week-old female BALB/c nude mice were housed in sterile condition. The mice were injected subcutaneously in the right flank with Huh7 human hepatocellular carcinoma cells (1×10^6/per). The carcinoma cell marker CD24 was examined by Immunohistochemistry (IHC; Supplementary materials and methods) when the tumors reached volume of 50–90 mm^3. The staining positivety of cells was defined as a membranous staining (anti-CD24) with brown, and the tumors were given a semiquantitative score: 0, <50% (+), >50% (++), or 100% (+++) positive carcinoma cells (Mordant et al., 2010).

2.11. Preparation of anti-CD24-MPA probes

Near-infrared fluorescent dye multiplex probe amplification (MPA) 7.98 mg and 2.11 mg (3-dimethylaminopropyl)-3-ethyl carbodiimide hydrochloride (EDC) were mixed and dissolved in 1 ml dimethylformamide (DMF). The resultant mixture was stirred in dark at room temperature for 2 h, followed by the addition of 1.38 mg *N*-hydroxysuccinimide (NHS) and 6 mg G7mAb or G7S and continued stirring in the dark for further 12 h. The products were then purified with Sephadex G-75 molecular sieve column and washed with PBS buffer (pH 8.0) before collecting the blue ribbons anti-CD24-MPA probes, namely G7mAb-MPA and G7S-MPA.

2.12. Dynamics and targeted ability of G7mAb-MPA and G7S-MPA in tumor bearing mice

A total of 20 mice used in this study were divided into four groups. Two groups of mice were tail-intravenously injected with 100 μl of 50 μmol/L anti-CD24-MPA probes G7mAb-MPA or G7S-MPA respectively. To evaluate the targeting of the probes, two groups of mice were tail-intravenously injected with anti-CD24-MPA probe and the free corresponding antibody (mole ratio = 1:50), which are blocking exprientment groups. Near-infrared camera was used to take photos of each group at different time intervals (0.5, 2, 4, 6, 12, and 24 h) after injection. Mice were focused radiated with NL-FC-2.0-763 type semiconductor laser, PIXIS512B type CCD camera collecting the fluorescence signal in real time. The whole process was carried out in a darkroom to reduce interference of background light. The tumor/normal tissue ratios (T/N ratio) were analyzed by analysis region of interests (ROI) function.

2.13. Statistical analysis

Data are presented as the mean ± SD. Student's *t*-test was used to evaluate the different between groups. $P < 0.05$ was considered statistically.

3. Results

3.1. Construction, expression and purification of CD24-GST

A recombinant fusion protein consisting of 33 amino CD24 core and GST tag was designed as immunogen (Fig. 1A). By inducing the expression system (*E. coli* BL21 (DE3)/pGEX-hCD24) with IPTG, the fusion protein was successfully expressed. The western blotting assay (Fig. 1B) demonstrated that CD24-GST fusion protein can specifically recognized by GST tag antibody. The target protein (CD24-GST) was purified with affinity chromatography and verified by SDS-PAGE. The molecular weight of the purified protein was 30 kD and was consistent with the predicted molecular weight (Fig. 1C).

3.2. Immunization, production and purification of G7mAb

The three mice serum titers reached 1:20000 after immunization process was completed (Fig. 2A). The impact immunization of the mouse of the highest serum efficiency value which happened to mouse number 2 (#2) yielded serum titer of 1:80000 (Fig. 2B). Screening hybridroma (spleen of mouse #2 fused with Sp20-Ag14 myeloma cells) with ELISA for the production of antibodies against CD24 polypeptides showed that 62 wells were positive (Data not shown). Stable clone secreting anti-CD24 antibody was obtained after three rounds of screening and its ELISA

Please cite this article in press as: He, H., et al., A novel antibody targeting CD24 and hepatocellular carcinoma *in vivo* by near-infrared fluorescence imaging. Immunobiology (2015), http://dx.doi.org/10.1016/j.imbio.2015.07.010

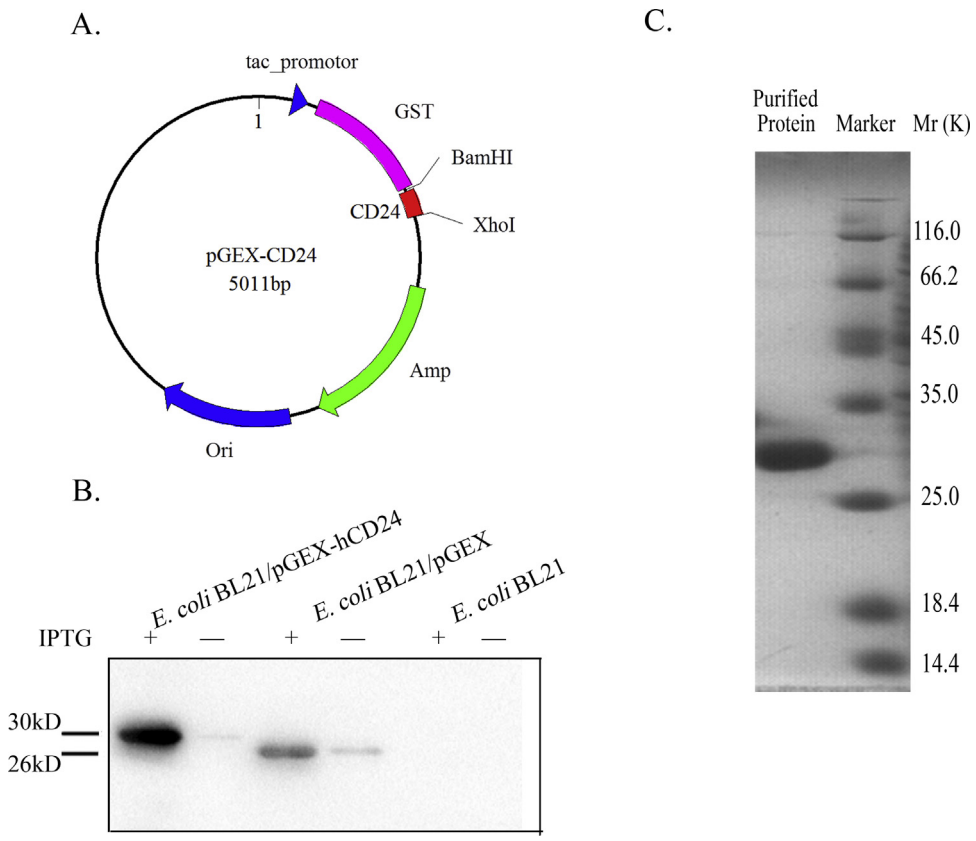

Fig. 1. Generation and purification of the recombinant antigen CD24.
(A) Map of the recombinant plasmid vector pGEX-hCD24. (B) Evaluation of a successful construction and expression of the fusion protein GST-CD24 using western blot assay with anti-GST antibody. Lane 1: *E. coli* BL21/pGEX-hCD24 (induced with IPTG); Lane 2: *E. coli* BL21/pGEX-hCD24 (non-induced); Lane 3: *E. coli* BL21/pGEX (induced with IPTG); Lane 4: *E. coli* BL21/pGEX (non-induced); Lane 5: *E. coli* BL21 (induced with IPTG); Lane 6: *E. coli* BL21 (non-induced). (C) Coomassie-stained SDS-PAGE analysis of the purified GST-CD24 (30 kD).

positive rate reached 95%. Using the isotyping kit, G7mAb was identified to be the IgG1κisotype. Highly concentrated G7mAb was prepared from ascetic fluid of BALB/c mice and purified by Protein G affinity chromatography based on its isotype and the purity and molecular weight of G7mAb determined with SDS-PAGE analysis. The purified G7mAb had two bands corresponding to the heavy chain (50 kD) and the light chain (25 kD) (Fig. 2C) and purity was estimated to be greater than 95%.

3.3. Specificity analysis of G7mAb

G7mAb specifically detected recombinant human CD24 (CD24-Fc), but not the unrelated recombinant protein Fc. Anti-Fc antibody was used as control antibody. The results suggested that G7mAb can specifically be used to detect CD24 by western blotting (Fig. 3A). Also, in the Friguet assay, increasing concentration of competitive antigen resulted in a decrease in the reacting value (Fig 3B), also demonstrating the binding between G7mAb and CD24 peptide. Further, flow cytometry assay was carried out to assess the affinities of G7mAb to native CD24 expressed on Huh7 and HT29 cells with HCT116 cells as control. G7mAb demonstrated significant binding to both Huh7 and HT29 cells with rates 52.9% and 41.3% respectively, as against 99.7% of ML5 (control) (Fig. 3C).

3.4. Analysis of the G7mAb variable genes

The encoding cDNA sequence of the variable regions of the heavy and light chain proteins of about 330 bp were effectively amplified with degenerated PCR (Fig. 4A). The positive clones of VH and VL were screened with colony PCR (Date not shown). DNA sequencing showed that sequences of VH and VL were 339 bp and 336 bp respectively (SANGON, Shanghai, China). Then we loaded the protein sequences of VH and VL into the IMGT database, and the CDR1-3 and FR1-4 of VH and VL analyzed with IMGT/V-QUEST Tool demonstrated that the conserved amino acids have the correct position and consistent with antibody structural features(Fig. 4B).

3.5. Preparation, purification, ELISA and FACS of G7S

To construct the scFv gene, the VH and VL genes were assembled with linker DNA linked the genes and cloned into pET22b(+) vector by NcoI and NotI double restriction endonuclease digesting (Fig. 5A). In pET22b(+)-G7S, the scFv gene was inserted in-frame between a pelB leader sequence and a hexahistidine tag of pET22b(+). The recombinant vector was transformed into *E. coli* BL21 (DE3) and the expression system *E.coli* BL21 (DE3)/pET22b(+)-G7S for G7S expression was successfully constructed. SDS-PAGE and western blot assay effectively showed the expression of G7S with the appropriate molecular weight of 27 kD (Fig. 5B). The binding ability of G7S was determined with indirect ELISA and it showed a dose dependent binding affinity with GST-CD24 whereas non-significant binding affinity to the control proteins BSA and GST (Fig. 5C). G7S exhibited relatively lower binding affinity to both Huh7 and HT29 cells with rates 8.88% and 9.23% respectively. G7S showed non-significant binding affinity to HCT116 cells (0.160% and 0.100%) (Fig. 5D).

Please cite this article in press as: He, H., et al., A novel antibody targeting CD24 and hepatocellular carcinoma *in vivo* by near-infrared fluorescence imaging. Immunobiology (2015), http://dx.doi.org/10.1016/j.imbio.2015.07.010

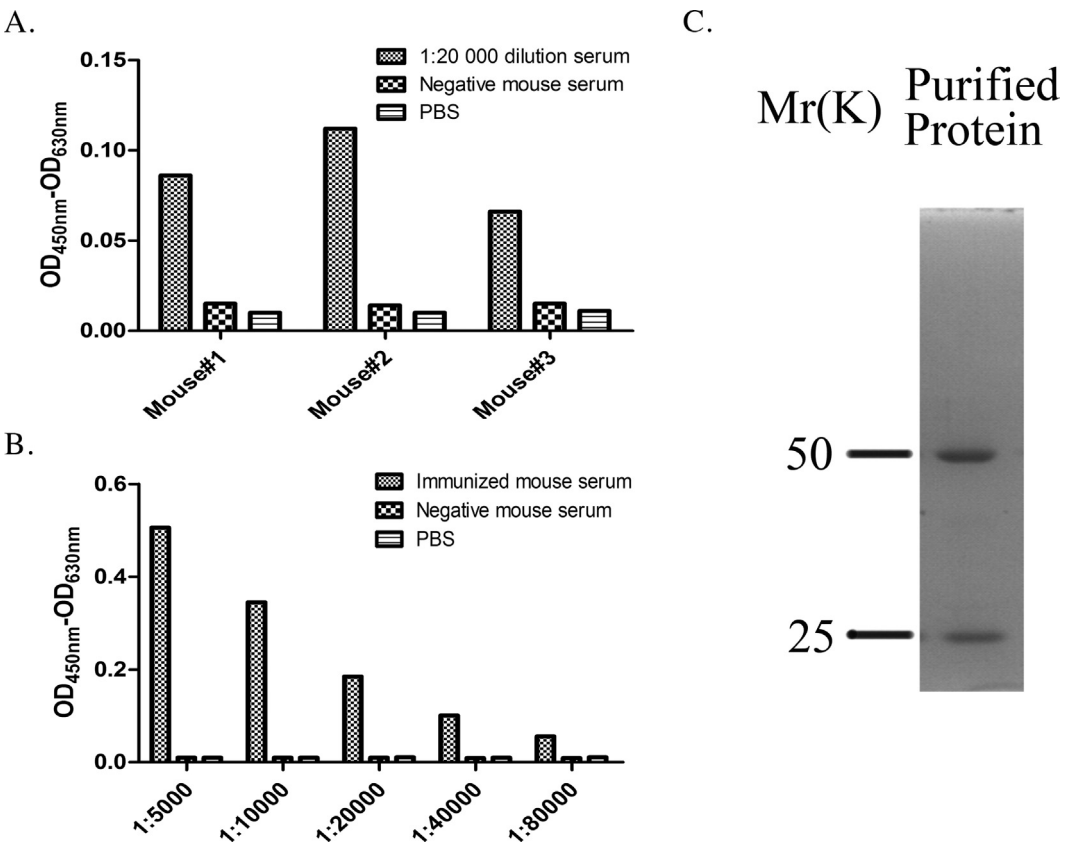

Fig. 2. Generation of G7mAb.
(A) Immunization of three mice and selecting the mouse with the best serum titre. The #2 mouse was selected for the impact immunization. (B) The serum titer of #2 mouse reached 1:80000 after the impact immunization. (C) Coomassie-stained SDS-PAGE analysis of the purified G7mAb.

3.6. Immunohistochemistry

The possibility of establishing the correct animal model and using G7mAb in immunohistochemistry were determined by staining the tumor samples from Huh7 xenograft nude mice with the ML5, G7mAb, and isotype antibody (negetive control). G7mAb specifically stained tumor samples just like the positive antibody ML5 (Fig. 6A), and demonstrated that the animal models for *in vivo* targeted assay were successfully established and G7mAb can be used in immunohistochemistry.

3.7. Dynamics and targeted ability of G7mAb and G7S in tumor bearing mice

This was done to assess the targeted ability of G7mAb and G7S *in vivo*. The anti-CD24-MPA probes (G7mAb-MPA and G7S-MPA) and the established animal models were used for the study. After the injection of G7mAb-MPA, the fluorescence signals diffused immediately to every part of the mice body and assembled distinctly in the right flank in 4 h, with maximal tumor/normal tissue ratio of 2.23 (Fig. 6D). Meanwhile, the blocking control group showed no intense fluorescence signals in the tumor tissues at the right flank (Fig. 6B), with maximal tumor/normal tissue ratio of 1.13 (Fig. 6D). A similar result was observed with G7S-MPA (Fig. 6C), with maximal tumor/normal tissue ratio of G7S-MPA treated group and the blocking group as 2.80 and 1.18 at 4 h, respectively (Fig 6D). These results indicate that G7mAb and G7S effectively targeted the tumor tissues by specifically binding to CD24 *in vivo*.

4. Discussion

The HCC has reportedly shown poor prognosis, and low response rate to chemotherapy and radiotherapy (Levin and Amos, 1995; Belnoue et al., 2004). And considering the fact that most patients usually report with advanced condition at diagnosis, surgery is also not possible due to the underlying cirrhosis (Bruix and Sherman, 2005; Lorenz et al., 2000; Matar et al., 2009). Nevertheless, novel strategy such as targeted therapy which is an aspect of immunotherapy has proven potent in the treatment of HCC (Butterfield et al., 2007; Gao et al., 2007; Kobayashi et al., 2007; Peng et al., 2005). This normally involves the use of monoclonal antibodies and small molecule inhibitors.

We developed CD24 specific monoclonal antibody G7mAb through hybridoma technology and generated single-chain antibody fragment (scFv) against CD24 (G7S) based on G7mAb. The suitability of the antibody (G7mAb) being used for western blot assay, ELISA and flow cytometry assay was evaluated. G7mAb showed specific binding affinity to recombinant human CD24 but not to unrelated recombinant Fc by western blot. This suggests that G7mAb can be used in western blot to detect CD24 (Fig. 3A). The competitive ELISA test also confirmed the specificity of the binding between G7mAb and the antigen CD24 and fact that G7mAb can be used in ELISA test (Fig. 3B). As presented on Fig. 5C, G7S also exhibited specific binding affinity to CD24. The affinity was dose dependent, increased with increasing concentration of G7S. Their affinity to CD24 was further confirmed by flow cytometry assay with $CD24^{+}$ Huh7 and HT29 (Figs. 3 C and 5 D). Both showed binding affinity to native CD24 but the affinity of G7mAb was relatively stronger than that of G7S. This is not a surprising outcome, because the binding rate of scFv derived from full antibody usually

Please cite this article in press as: He, H., et al., A novel antibody targeting CD24 and hepatocellular carcinoma *in vivo* by near-infrared fluorescence imaging. Immunobiology (2015), http://dx.doi.org/10.1016/j.imbio.2015.07.010

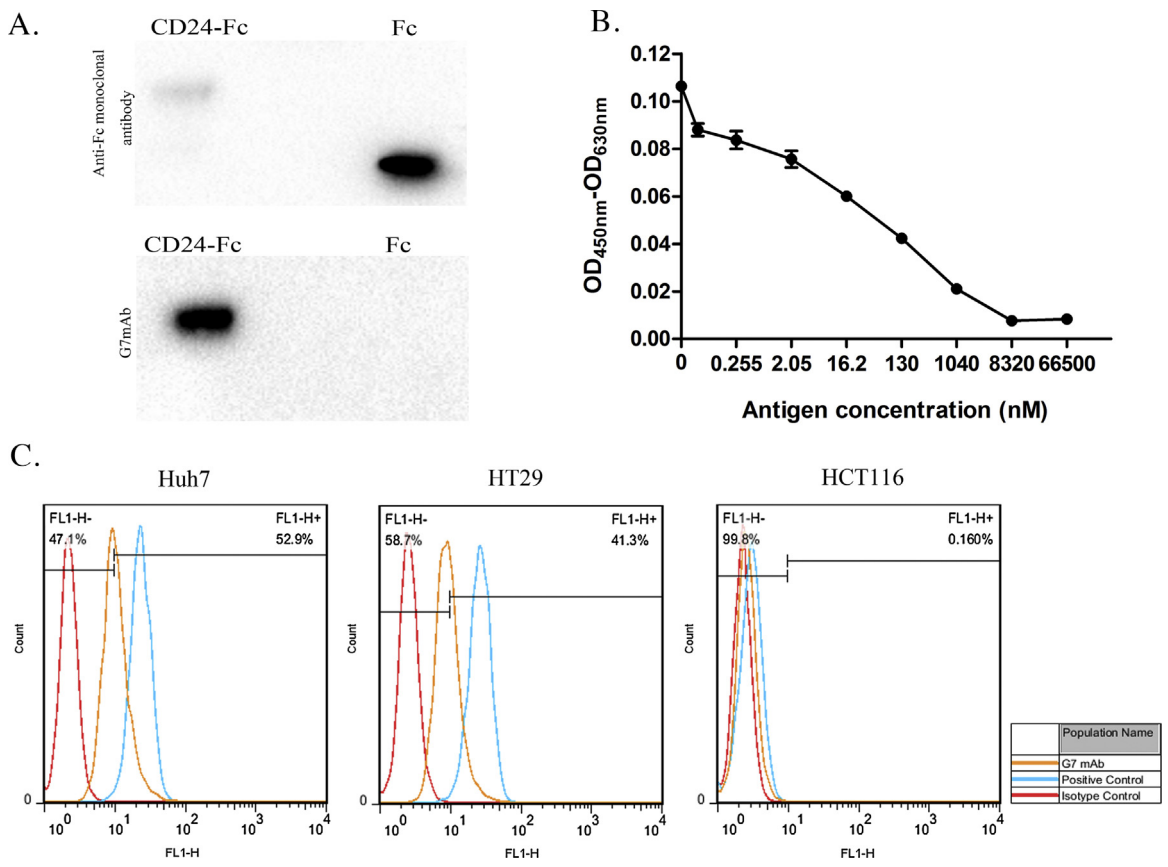

Fig. 3. Analyzing the specificity of G7mAb.
(A) Western blot assay of CD24 (CD24-Fc) or Fc detected by G7mAb. G7mAb specifically detected the recombinant human CD24 (CD24-Fc) but not the unrelated recombinant protein Fc. (B) Friguet determination of G7mAb affinity. The curve of competitive ELISA suggests that G7mAb has specific affinity for recombinant CD24. (C) Analyzing the affinity of binding G7mAb with native CD24 expressed on Huh7 and HT29. The binding rates of G7mAb with Huh7 and HT29 were 52.9% and 41.3% respectively. However, it showed no binding affinity with the CD24-negative control cell line HCT116.

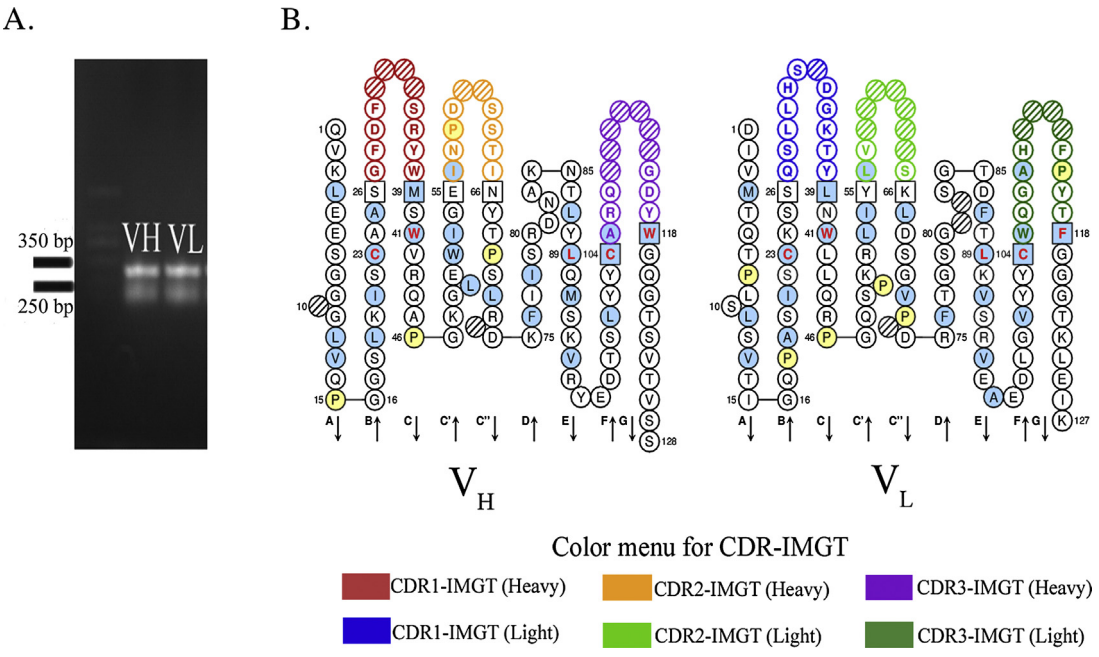

Fig. 4. Analysis of the G7mAb variable genes.
(A) Agarose gel electrophoresis of VH and VL genes (about 330 bp each). (B) The schematic diagram of the functional domains of VH and VL of G7mAb. The conserved amino acids are at the correct position, consistent with antibody structural features.

Please cite this article in press as: He, H., et al., A novel antibody targeting CD24 and hepatocellular carcinoma *in vivo* by near-infrared fluorescence imaging. Immunobiology (2015), http://dx.doi.org/10.1016/j.imbio.2015.07.010

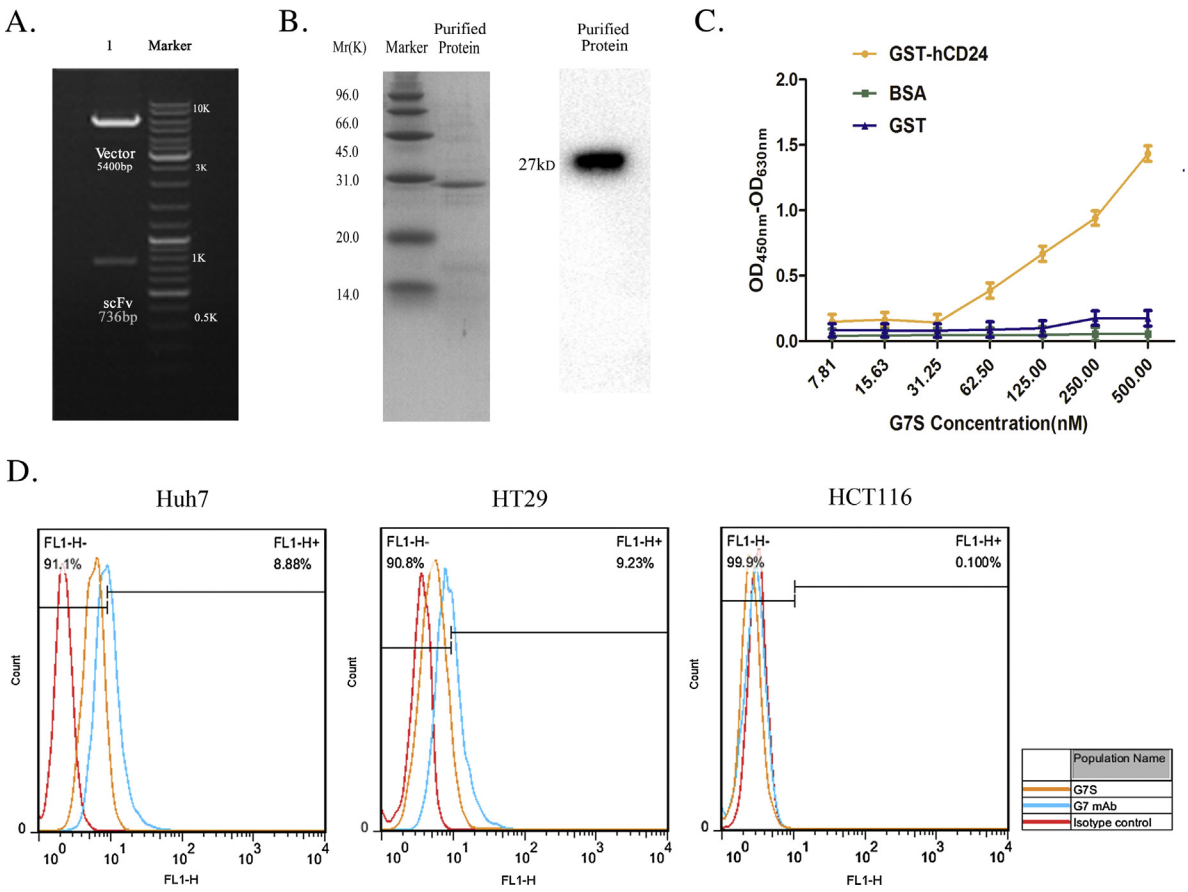

Fig. 5. Generation, purification and the binding specificity evaluation of G7S.
(A) Double digestion of the recombinant plasmid pET22b-G7S with *NcoI* and NotI. Lane 1: digested plasmid and G7S (736 bp); Lane 2: marker. (B) Coomassie-stained SDS-PAGE (left) and western blot analyses (right) of G7S expression. (C) G7S demonstrated dose dependent binding affinity to recombinant GST-CD24. (D) Analyzing the biding affinity of G7S to native CD24 expressed on Huh7 and HT29. The binding rates of G7S to Huh7 and HT29 were 8.88% and 9.23% respectively. However, it showed no binding affinity to the CD24-negative control cell line HCT116.

declines (Carter, 2006; Sliwkowski and Mellman, 2013). G7S lacked Fc region, so its affinity reduced. In addition, G7S was expressed by prokaryotic expression system, therefore it lacked glycosylation which influenced its affinity. In the flow cytometry assays, cells were washed three times. The strong centrifugal force would therefore cause part of the bound G7S to be shed, which would possibly led to lower binding rate of G7S. The affinity of G7mAb was then compared with ML5 (a commercial Anti-CD24 Mouse Antibody) to determine its strength. The binding rate of G7mAb was 52.9% whereas the ML5 recorded a higher rate of 99.7% with the $CD24^+$ Huh7 cells. This huge disparity could be due to the fact that the immunogen of G7mAb (GST-CD24) was expressed with prokaryotic expression system. Therefore, the possible lack of glycosylation in GST-CD24 and its spatial conformation could account for this. Thus the binding of G7mAb with CD24 over-expressed cell lines is not ideal.

However, in immunohistochemistry, G7mAb and ML5 exhibited relatively similar binding capacity (Fig. 6A). The reason is that, the samples deal with organic reagent, and the fact that the linear epitope of CD24 expressed on the surface of the cells is exposed, makes it conducive for G7mAb to bind. This therefore suggests that G7mAb be used in immunohistochemical assay.

Near-infared fluorescence is a kind of molecular imaging. It relies on bio-compatible, specific fluorescent probes and proteins to quantitate and visualize targets, biological processes, and cells *in vivo* noninvasively (Filonov et al., 2011; Hilderbrand and Weissleder, 2010; Ntziachristos et al., 2003). The targeted capacity of the antibodies (G7mAb and G7S) were investigated *in vivo* with $CD24^+$ Huh7 hepatocellular carcinoma xenograft tissue by near-infrared fluorescence imaging using anti-CD24-MPA (G7mAb-MPA and G7S-MPA) probes. And as presented on Fig 6B and C, G7mAb-MPA and G7S-MPA effectively targeted the tumor tissues *via* specific binding to CD24 *in vivo*. These suggest that, G7mAb and G7S exhibited specific binding affinity to CD24 molecules on cellular surface, and to CD24 expressed on tumor tissue *in vivo*. After injection of G7S-MPA, the intense sinal at tumor sites was maintained up to 6 h, with the tumor/normal tissue ratio of 2.18 (Data not shown), but the intense signal at tumor sites was weak at 6 h after injection of the G7mAb-MPA, with the tumor/normal tissue ratio of 1.36 (Data not shown). Although, the *in vitro* antigen-binding capacity of G7S was relatively weak compared to G7mAb (Figs. 3 C and 5 D), its ability to bind *in vivo* was better than G7mAb. Because G7S has smaller molecular weight (27 kD) compared to the 150 kD of G7mAb, and also retained the antigen binding site and affinity to the imprinted molecules. G7S therefore has a better ability to penetrate the tumor tissue than the heavier G7mAb.

In summary, we developed CD24 targeted monoclonal antibody G7mAb through hybridoma technology and generated single-chain antibody fragment (scFv) against CD24 (G7S) based on G7mAb, which exhibited tumor targeted therapeutic and diagnostic potentials *in vitro* and *in vivo*. Based on the specificity and tumor targeting of G7mAb and G7S, toxins can be conjugated to the antibodies in future, making antibody-drug conjugates, to improve the targeted ability to toxins and reduce toxic effect to the body. Antibody-drug

Please cite this article in press as: He, H., et al., A novel antibody targeting CD24 and hepatocellular carcinoma *in vivo* by near-infrared fluorescence imaging. Immunobiology (2015), http://dx.doi.org/10.1016/j.imbio.2015.07.010

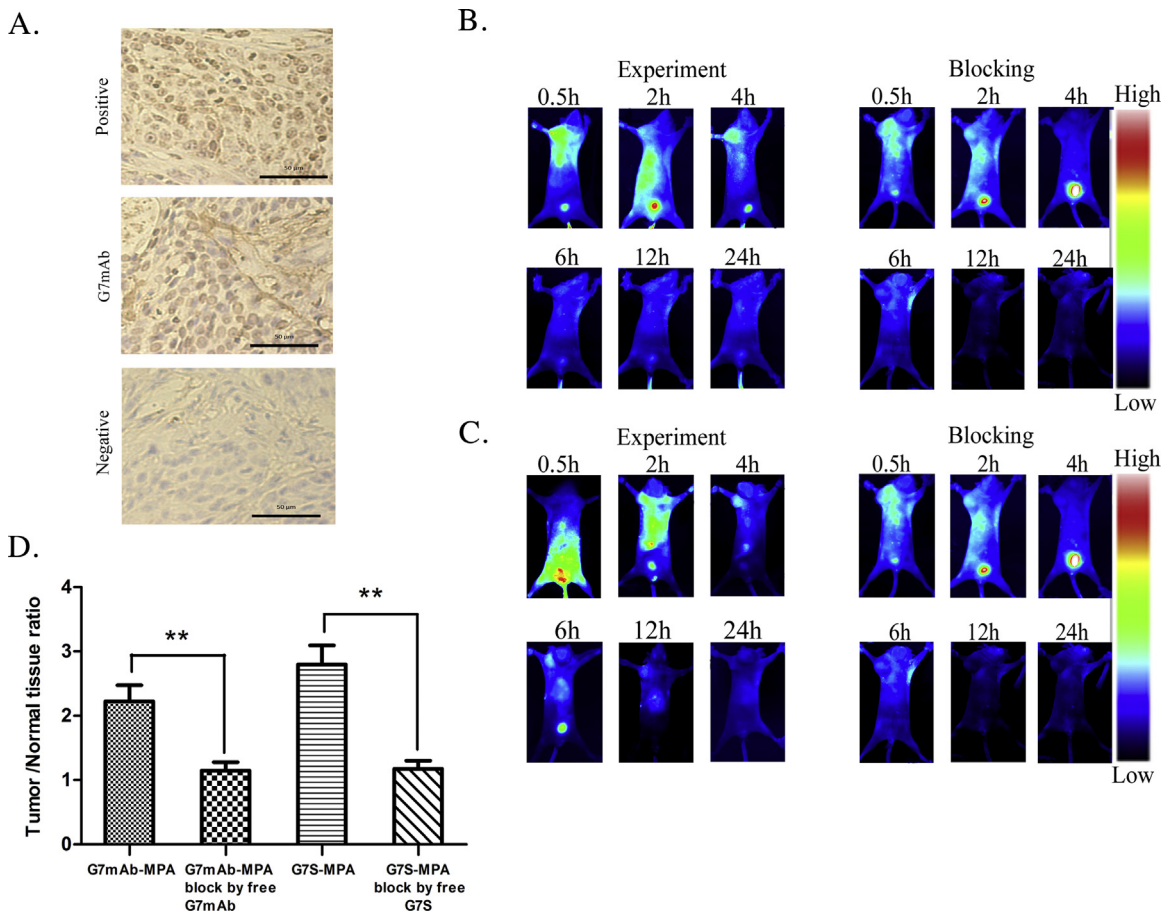

Fig. 6. Tumor targeted efficacy of G7mAb and G7S.
(A) The immunohistochemical results of CD24 on Huh7 xenograft tumor model with G7mAb. The staining positivety of tumor cells was defined as a membranous staining with an anti-CD24 antibody ML5 (positive control): strong brown staining, semiquantitative score of >50% (++) positive tumor cells. The staining positivety with G7mAb: moderate brown staining, semiquantitative score of >50% (++) positive tumor cells. There was no membranous staining in the negative control. (B, C) Near-infrared spectroscopy of tumor-bearing mice. (B) G7mAb -MPA and (C) G7S-MPA effectively targeted the tumor tissues via specific binding to CD24 *in vivo*, although G7S proved more efficient than G7mAb. (D) Maximal tumor/normal tissue ratio {T/N ratio = [tumor sinal background signal]/[normal signal (muscle) background signal] × 100%} calculated from the ROIs at 4-h post-injection. Data are given as mean ± SD ($n = 5$). Significance is indicated by asterisks ($^{**}P < 0.01$).

conjugates can improve the treatment effect and reduce the pain of patients, so they have application prospect and direct our future research.

Conflict of interest

The authors declare that they have no conflict of interest.

Acknowledgments

This work was supported by the National Natural Science Foundation of China (NSFC81273425 and NSFC81473125) and Specialized Research Fund for the Doctoral Program of Higher Education (20130096110007). China Scholarship Council and Jiangsu Province Qinglan Project (2014). A Project Funded by the Priority Academic Program Development of Jiangsu Higher Education Institutions.

Appendix A. Supplementary data

Supplementary data associated with this article can be found, in the online version, at http://dx.doi.org/10.1016/j.imbio.2015.07.010

References

Belnoue, E., Guettier, C., Kayibanda, M., Le Rond, S., Crain-Denoyelle, A.M., Marchiol, C., et al., 2004. Regression of established liver tumor induced by monoepitopic peptide-based immunotherapy. J. Immunol. 173 (8), 4882–4888.
Berzofsky, J.A., Terabe, M., Oh, S., Belyakov, I.M., Ahlers, J.D., Janik, J.E., Morris, J.C., 2004. Progress on new vaccine strategies for the immunotherapy and prevention of cancer. J. Clin. Invest. 113 (11), 1515–1525.
Bruix, J., Sherman, M., 2005. Management of hepatocellular carcinoma. Hepatology 42 (5), 1208–1236.
Butterfield, L.H., Ribas, A., Potter, D.M., Economou, J.S., 2007. Spontaneous and vaccine induced AFP-specific T cell phenotypes in subjects with AFP-positive hepatocellular cancer. Cancer Immunol. Immunother. 56 (12), 1931–1943.
Carter, P.J., 2006. Potent antibody therapeutics by design. Nat. Rev. Immunol. 6 (5), 343–357.
Deng, J., Gao, G., Wang, L., Wang, T., Yu, J., Zhao, Z., 2012. CD 24 expression as a marker for predicting clinical outcome in human gliomas. Biomed. Res. Int.
El-Serag, H.B., Rudolph, K.L., 2007. Hepatocellular carcinoma: epidemiology and molecular carcinogenesis. Gastroenterology 132 (7), 2557–2576.
Filonov, G.S., Piatkevich, K.D., Ting, L.M., Zhang, J., Kim, K., Verkhusha, V.V., 2011. Bright and stable near-infrared fluorescent protein for *in vivo* imaging. Nat. Biotechnol. 29 (8), 757–761.
Gao, Q., Qiu, S.J., Fan, J., Zhou, J., Wang, X.Y., Xiao, Y.S., et al., 2007. Intratumoral balance of regulatory and cytotoxic T cells is associated with prognosis of hepatocellular carcinoma after resection. J. Clin. Oncol. 25 (18), 2586–2593.
Gerber, D.E., 2008. Targeted therapies: a new generation of cancer treatments. Am. Fam. Physician 77 (3), 311–319.
Gilboa, E., 2004. The promise of cancer vaccines. Nat. Rev. Cancer 4 (5), 401–411.
Hilderbrand, S.A., Weissleder, R., 2010. Near-infrared fluorescence: application to *in vivo* molecular imaging. Curr. Opin. Chem. Biol. 14 (1), 71–79.

Hough, M.R., Rosten, P.M., Sexton, T.L., Kay, R., Humphries, R.K., 1994. Mapping of CD24 and homologous sequences to multiple chromosomal loci. Genomics 22 (1), 154–161.
Huang, L.R., Hsu, H.C., 1995. Cloning and expression of CD24 gene in human hepatocellular carcinoma: a potential early tumor marker gene correlates with p53 mutation and tumor differentiation. Cancer Res. 55 (20), 4717–4721.
Karimi-Busheri, F., Rasouli-Nia, A., Zadorozhny, V., Fakhrai, H., 2013. CD24+/CD38-as new prognostic marker for non-small cell lung cancer. Multidiscip. Respir. Med. 8 (1), 65.
Kobayashi, N., Hiraoka, N., Yamagami, W., Ojima, H., Kanai, Y., Kosuge, T., et al., 2007. FOXP3+ regulatory T cells affect the development and progression of hepatocarcinogenesis. Clin. Cancer Res. 13 (3), 902–911.
Kristiansen, G., Pilarsky, C., Pervan, J., Stürzebecher, B., Stephan, C., Jung, K., et al., 2004. CD24 expression is a significant predictor of PSA relapse and poor prognosis in low grade or organ confined prostate cancer. Prostate 58 (2), 183–192.
Lee, T.K.W., Castilho, A., Cheung, V.C.H., Tang, K.H., Ma, S., Ng, I.O.L., 2011. $CD24^{+}$ liver tumor-initiating cells drive self-renewal and tumor initiation through STAT3-mediated NANOG regulation. Cell Stem Cell 9 (1), 50–63.
Levin, B., Amos, C., 1995. Therapy of unresectable hepatocellular carcinoma. N. Engl. J. Med. 332 (19), 1294–1296.
Lim, S.C., 2005. CD24 and human carcinoma: tumor biological aspects. Biomed. Pharmacother. 59, S351–S354.
Liu, C., Zheng, S., Shen, H., Xu, K., Chen, J., Li, H., et al., 2013. Clinical significance of CD24 as a predictor of bladder cancer recurrence. Oncol. Lett. 6 (1), 96–100.
Lorenz, M., Staib-Sebler, E., Hochmuth, K., Heinrich, S., Gog, C., Vetter, G., Encke, A., Muller, H.H., 2000. Surgical resection of liver metastases of colorectal carcinoma: short and long-term results. Semin. Oncol. 27, 112–119.
Maor, Y., Malnick, S., 2013. Liver injury induced by anticancer chemotherapy and radiation therapy. Int. J. Hepatol. 2013, 8, http://dx.doi.org/10.1155/2013/815105, Article ID 815105.
Matar, P., Alaniz, L., Rozados, V., Aquino, J.B., Malvicini, M., Atorrasagasti, C., et al., 2009. Immunotherapy for liver tumors: present status and future prospects. J. Biomed. Sci. 16 (30), 1–18.
Mordant, P., Loriot, Y., Leteur, C., Calderaro, J., Bourhis, J., Wislez, M., et al., 2010. Dependence on phosphoinositide 3-kinase and RAS-RAF pathways drive the activity of RAF265, a novel RAF/VEGFR2 inhibitor, and RAD001 (Everolimus) in combination. Mol. Cancer Ther. 9 (2), 358–368.
Ntziachristos, V., Bremer, C., Weissleder, R., 2003. Fluorescence imaging with near-infrared light: new technological advances that enable *in vivo* molecular imaging. Eur. Radiol. 13 (1), 195–208.
Peng, B.G., Liang, L.J., He, Q., Kuang, M., Lia, J.M., Lu, M.D., Huang, J.F., 2005. Tumor vaccine against recurrence of hepatocellular carcinoma. World J. Gastroenterol. 11 (5), 700–704.
Schostak, M., Krause, H., Miller, K., Schrader, M., Weikert, S., Christoph, F., et al., 2006. Quantitative real-time RT-PCR of CD24 mRNA in the detection of prostate cancer. BMC Urol. 6 (1), 7.
Shapira, S., Shapira, A., Starr, A., Kazanov, D., Kraus, S., Benhar, I., Arber, N., 2011. An immunoconjugate of Anti-CD24 and *Pseudomonas* exotoxin selectively kills human colorectal tumors in mice. Gastroenterology 140 (3), 935–946.
Sliwkowski, M.X., Mellman, I., 2013. Antibody therapeutics in cancer. Science 341 (6151), 1192–1198.
Soave, D.F., da Costa, J.P.O., da Silveira, G.G., Ianez, R.C.F., de Oliveira, L.R., Lourenço, S.V., Ribeiro-Silva, A., 2013. CD44/CD24 immunophenotypes on clinicopathologic features of salivary glands malignant neoplasms. Diagn. Pathol. 8 (1), 29.
Wang, Z., Raifu, M., Howard, M., Smith, L., Hansen, D., Goldsby, R., Ratner, D., 2000. Universal PCR amplification of mouse immunoglobulin gene variable regions: the design of degenerate primers and an assessment of the effect of DNA polymerase 3′ to 5′ exonuclease activity. J. Immunol. Methods 233 (1), 167–177.
Weichert, W., Denkert, C., Burkhardt, M., Gansukh, T., Bellach, J., Altevogt, P., et al., 2005. Cytoplasmic CD24 expression in colorectal cancer independently correlates with shortened patient survival. Clin. Cancer Res. 11 (18), 6574–6581.

Please cite this article in press as: He, H., et al., A novel antibody targeting CD24 and hepatocellular carcinoma *in vivo* by near-infrared fluorescence imaging. Immunobiology (2015), http://dx.doi.org/10.1016/j.imbio.2015.07.010